

# Framework for Coupling Room Air Models to Heat Balance Model Load and Energy Calculations (RP-1222)

**Brent Griffith**

**Qingyan (Yan) Chen, Ph.D.**

Member ASHRAE

---

*Most energy and load calculation procedures have assumed that room air is well mixed, which may lead to significant errors in sizing HVAC systems, estimating building energy use, and predicting thermal comfort for buildings with buoyancy-driven room airflow. This investigation has developed a framework and computer code for coupling detailed air models with building energy and load calculations as an extension to the ASHRAE Toolkit for Building Load Calculations. Two nodal models and a momentum-zonal model were selected for testing the coupling framework in a program for hourly load calculations of a single thermal zone. The heat balance model for load and energy calculations is reformulated to use zone air temperature as a variable defined separately for each surface. Air system flow rates are determined using air model predictions for temperature at the air system returns and a room air control location. The effect of air models on sensible load was found to be minor except when aggressive diurnal thermal mass strategies were involved. Nodal models appear practical to implement in load and energy programs and should improve results for air system flow rate and return air temperatures. Results show increases of about a factor of four in computing time for nodal models compared to the well-mixed model. Computing time is increased by two orders with the three-dimensional momentum-zonal model.*

---

## INTRODUCTION

Energy and load calculation procedures have relied for some thirty years on the assumption that zone air is thoroughly mixed. The application of a single control volume with a uniform zone air temperature at any point in time is reasonable for typical forced air system configurations where relatively good mixing is a design intent. The “well-stirred” zone model might be inadequate for some system designs or operating modes including:

- Air system off
- Displacement ventilation
- Underfloor air distribution
- Chilled beams
- Natural ventilation
- Mixed-mode ventilation
- Baseboard and convective heating
- Large or tall spaces, such as atria, auditoria, and stairwells

---

**Brent Griffith** is a senior engineer at the Center for Buildings and Thermal Systems, National Renewable Energy Laboratory, Golden, Colo., and **Qingyan (Yan) Chen** is a professor of mechanical engineering at Ray W. Herrick Laboratories, School of Mechanical Engineering, Purdue University, West Lafayette, Ind.

In such situations, the airflow in the indoor spaces cause nonuniform zone air temperatures. Some designs require the nonuniformity of the zone air temperature to improve energy efficiency and/or indoor air quality. Building rating systems need fair and accurate methods of comparing energy efficiency of alternative designs to conventional forced-air systems. Current trends of increased use of underfloor air distribution and natural or hybrid ventilation may create a need for engineers to account for their unique performance characteristics in sizing equipment and estimating energy use. To address these needs, it is important to estimate the impact of nonuniform distribution of indoor air temperature on the building load and energy simulations. It is therefore desirable to combine air modeling with load calculations.

Coupling air and load routines is not new. Detailed zone models of the thermal network type are available with both mass and energy balances and already offer the capabilities envisaged here (Sowell 1991; Walton 1993). These models represent the thermal zone with both surfaces and air nodes in a single network and present a single representation of the thermal zone to an HVAC component simulation. Researchers and engineers have long had the ability to formulate detailed network models of a thermal zone and solve them using a variety of software tools such as SPARK (1997) or IDA (EQUA 2002).

On the other hand, computational fluid dynamics (or CFD) has been used to model building room airflow for nearly 30 years. Chen and van der Kooi (1988) and Negrao (1995) coupled CFD to a building load/energy simulation program and, later, Beausoleil-Morrison (2000) expanded these capabilities. Other coupling work between CFD and a load/energy program includes those from Srebric et al. (2000) and Zhai et al. (2002). As pointed out by Srebric et al. (2000), a direct coupling of CFD with an energy simulation program for hourly simulation of building performance over a year is too demanding computationally.

This investigation tries to systematically build up a framework that allows an easy combination of different air models with load and energy models. Figure 1 diagrams the classification of room air models used in this paper. Such models have been developed for more than 30 years and are plentiful. The goal of the framework is to allow using all such air models with the ASHRAE toolkit (Pedersen et al. 2001). Although the terms *nodal* and *zonal* are used interchangeably in the literature, for the purposes of this study a distinction is made between them. The distinction is basically one of how strictly and how resolved the geometry of the control volumes is defined. A “nodal” model treats the building room air as an idealized network of

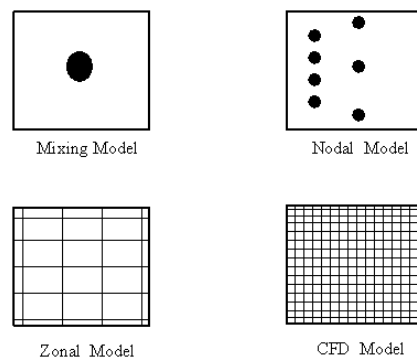


**Figure 1. Classification of room air models.**

nodes connected with flow paths. A “zonal” model uses a grid of well-defined control volumes. In both cases, energy balances are solved, but zonal models typically have many more fluid balance relations.

Three models were selected as examples for demonstrating and testing the coupling framework. Two of these are nodal models for sidewall displacement ventilation by Mundt (1996) and Rees (1998) or Rees and Haves (2001). The third is a simplified three-dimensional airflow model referred to as the momentum-zonal model (Griffith and Chen 2003). The CFD models are excluded from this study because of their high computing costs at present. However, the framework developed here is CFD-ready. CFD models can be easily plugged in should it become computationally affordable in the near future. Nevertheless, the air models themselves are not presented here in order to focus the discussion on a framework for use with any room air model, which forms the objective of the present investigation. More detailed information regarding different air models can be found in the literature (Rees and Haves 2001; Haghighat et al. 2001; Inard et al. 1996; Griffith and Chen 2003) and have been compared by Chen and Griffith (2002).

## FORMULATION

In formulating a framework for combined room air and load models, it is desirable that the framework be simple and applicable to a variety of room air models. The starting point for this effort is the original heat balance model in the ASHRAE toolkit (Pedersen et al. 1997; Pedersen et al. 2001). The new formulation alters the heat balance model wherever its model equations include variables for the zone air temperature. The air heat balance of the original model is considered an aggregate assessment of the air system’s change in enthalpy and is referred to as the “ $\dot{Q}_{sys}$ -equation.” The air and surface domains are modeled separately.

In addition to the single control volume for room air, additional subdivisions of this control volume are allowed for the purpose of modeling distributions of air temperature within the room. The air in the room is assumed to be a collection of separate, essentially well-mixed control volumes, where each is modeled as having the following:

1. uniform state conditions such as temperature and pressure,
2. constant properties such as density and specific heat,
3. transparency to radiation, and
4. uniform distributions of heat and mass transfer at each control volume boundary.

In aggregate, the room air control volumes must agree with an overall air system heat balance. Note that the assumptions for room air control volumes parallel those for surfaces:

1. uniform surface temperatures
2. uniform irradiation
3. diffusely emitted radiation
4. one-dimensional heat conduction within

There are five distinct processes:

1. outside face heat balance
2. wall conduction heat transfer
3. inside face heat balance
4. air system heat balance
5. air convective heat transport

Each inside face interacts with a specified control volume rather than all of them interacting with a single air control volume. The term “inside face” refers to the inside face of an enclosure surface (such as windows, walls, floor, ceiling) that faces the room air. The near-surface air is referred to as the *adjacent air control volume*. The additional fifth heat transfer process accounts

for convective energy transport arising from the movement of air between control volumes. Note that surface convective heat transfer is a different phenomenon than convective heat transport in the room air. Figure 2 is an adaptation of the “heat balance diagram,” showing the added detail of the present formulation.

### Implementing the Coupled Air and Load Models

Zhai and Chen (2003) concluded that stable solutions do in fact exist, and the advantages of coupling are preserved for the following coupling method. The air model generates values for the surface heat transfer coefficient and effective air temperature distribution and passes these to load/energy routines. The load/energy routines pass values for the surface temperature to the air model. This method is selected by the present investigation as a guiding principle for the framework’s treatment of the surface/air boundary.

The heat balance processes for a thermal zone can be formulated in a manner consistent with the formulation described by Pedersen et. al. (2001). No changes are made to the surface conduction processes or the outside face heat balance, so the equation for outside face surface temperature is the same. Transient heat transfer through the surface construction is modeled using a

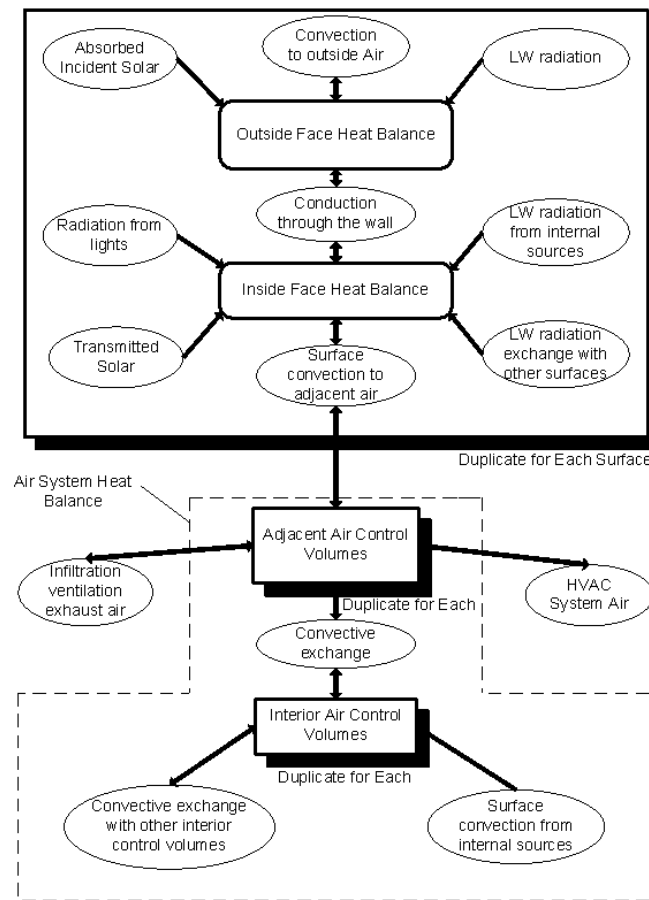


Figure 2. Schematic of heat balance processes in a zone with air models.

time series method called conduction transfer function, or CTF, for computational efficiency at hourly time steps. The inside face temperature and the system load are modified by rewriting the zone air temperature,  $T_a$ , with an additional subscript,  $i$ , for the surface index ( $T_a \rightarrow T_{a_{i,j}}$  or  $T_a \rightarrow T_{a_i}$ ). The inside face heat balance is solved for its surface temperature (see Pedersen et. al. [2001] for more explanation).

$$T_{s_{i,j}} = \frac{T_{so_{i,j}} Y_{i,o} + \sum_{k=1}^{nz} T_{so_{i,j-k}} Y_{i,k} - \sum_{k=1}^{nz} T_{s_{i,j-k}} Z_{i,k} + \sum_{k=1}^{nq} \Phi_{i,k} q''_{ki_{i,j-k}} + T_{a_{i,j}} h_{c_{i,j}} + q''_{LWS} + q''_{LWX} + q''_{SW} + q''_{sol}}{Z_{i,o} + h_{c_{i,j}}} \quad (1)$$

where

- $T_s$  = inside face temperature
- $i$  = subscript indicating individual surfaces
- $j$  = subscript indicating current time step
- $k$  = subscript indicating time history steps
- $T_{so}$  = outside face temperature
- $Y_i$  = cross CTF coefficients
- $Z_i$  = inside CTF coefficients
- $\Phi_i$  = flux CTF coefficients
- $q''_{ki}$  = conductive heat flux through the surface
- $h_{c_i}$  = surface convective heat transfer coefficient
- $T_a$  = near-surface air temperature
- $q''_{LWS}$  = longwave radiant heat flux from equipment in zone
- $q''_{LWX}$  = net long-wavelength radiant flux exchange between zone surfaces
- $q''_{SW}$  = net short wavelength radiant flux to surface from lights
- $q''_{sol}$  = absorbed direct and diffuse solar (short wavelength) radiation

The overall air system heat balance leads to the  $\dot{Q}_{sys}$ -equation,

$$\dot{Q}_{sys} = \sum_i A_i h_{c_i} (T_{s_{i,j}} - T_{a_{i,j}}) + \dot{Q}_{conv,S} + \dot{Q}_{Infil} \quad (2)$$

The zone air temperature is represented by an array of values that are of “primary” interest in a coupling surface and air models. The equations to generate values for  $T_{a_i}$  are part of the air model and depend on which air model is used. These models are not presented here since there is not yet a “preferred” air model. Rather, a framework for testing air models is developed that allows investigating their behavior.

### Direct vs. Indirect Coupling

In our framework for coupling, we have tried to present only a preferred methodology rather than a comprehensive survey of all the many different options. However, two groups of coupling options have emerged with complementary advantages. These two methods are termed “direct” and “indirect.” The major difference between them is that with indirect coupling, the room air is assumed to be controlled such that the air affecting the thermostat is at the desired setpoint. With direct coupling, there is no assumption of control or comfort, and values for  $T_a$  are obtained directly from the air model. With indirect-coupling, values for  $T_a$  are obtained from the air model as a relative distribution of differences and applied to the control setpoint in the

load/energy routines. The air model temperature difference used for indirect coupling is obtained from

$$\Delta T_{a_i} = (T_{a_i} - T_{statDB}), \quad (3)$$

where  $T_{statDB}$  is the air model's prediction at the location of the thermostat (computed by the air model). In the load routines, the value for  $T_a$  is then obtained from

$$T_{a_i} = T_{setpoint} + \Delta T_{a_i}, \quad (4)$$

where  $T_{setpoint}$  is the desired room air temperature (an input). Both of these coupling methods have been implemented as options in the toolkit source code and programs.

### Surface Convection

Improving the treatment of surface convection is one of the main reasons to implement such coupling, and additional discussion is warranted. Surface convection appears in heat balances in both the air and surface modeling domains so the simplest and safest approach is to use the same relation for  $\dot{Q}_c$  in both domains. So the usual model for convection surface heat transfer is written for each surface,

$$\dot{Q}_{c,i} = Ah_{c,i}(T_{s,i} - T_{a,i}). \quad (5)$$

The area,  $A$ , and surface temperature,  $T_s$ , are straightforward; however, the film coefficient,  $h_c$ , and the effective air temperature,  $T_a$ , are perhaps deceptively simple and are discussed in more detail below. The sign convention here is that positive surface convection heat transfer,  $\dot{Q}_c$ , indicates net heat flow from the surface to the air and therefore adds to the cooling load. Equation 5 is a *mean* relation for an individual surface, so values for  $T_a$ ,  $T_s$ , and  $h_c$  are averages appropriate for the surface. In the event that the resolution of the air model is finer than the surface model, the data should be averaged so that they conform to the surface area. This averaging is necessary since the underlying surface is treated as one-dimensional.

### Spatial Location for Determining Adjacent Air Temperature

Building rooms are enclosures and not semi-infinite fluid regions. Considering that  $T_a$  is a variable and not a constant, a framework for coupling air models to load/energy routines requires clear specification of how values for  $T_{a_i}$  are to be determined. This air temperature is also known as the reference temperature for convective heat transfer calculations, but the term "reference temperature" is avoided here because it implies fixing the value. For the well-mixed model, one obvious selection is that  $T_a$  should match the one available value (considered a good model of the average air temperature). With nodal models, each surface is associated with a particular node, and the result for temperature at that node is used for  $T_a$ . (Although all surfaces need to have a node associated with them, some nodes might be associated with interior control volumes and not directly affect surfaces.) For zonal and CFD air models with a grid of interior air control volumes, the basic question is what distance scale to use when determining  $T_a$ . A distance of 0.1 m (4 in.) into the air away from a building surface's inside face is selected as an appropriate geometrical scale for a point at which to determine  $T_a$ . The sensitivity of temperature results to this distance scale is presented below. This value is chosen in view of the following points:

- The point must be outside the inner thermal boundary layer.
- The point should not be too far outside the thermal boundary layer.
- The standard method for measuring component U-factors using hot box thermal test facilities measures bulk air temperatures at a distance greater than 0.075 m.
- A height of 0.1 m is often used for floor air temperature at ankle height.
- Zhai et al. (2002) used 0.1 m for coupling CFD with EnergyPlus.

### Surface Convection Coefficient

The surface convection heat transfer coefficient,  $h_c$ , is an important parameter. A convection correlation for building simulation may have been developed for use with the well-mixed assumption and so may have built-in dependence on both air movement and temperature near the wall. Beausoleil-Morrison (2000) developed a comprehensive methodology for selecting appropriate correlations to use for calculating  $h_c$  within a building simulation program. While the general approach remains valid, there is reason to suspect that correlations for  $h_c$  were developed for the well-mixed model's choice of  $T_a$  and may not apply as well to computations using near-surface values for  $T_a$ . Values for  $T_{a_i}$  from air models will often be closer to the temperature of the wall, requiring higher values of  $h_c$  to obtain the same heat flow rate. Spitler et al. (1991a, 1991b) developed convection coefficients from measurements for four different choices of reference temperature and found coefficients to vary from about 3.0 to 8.0 W/m<sup>2</sup>·K. Developing a new suite of correlations for  $h_c$  is beyond the scope of this investigation. Therefore, our interim approach is to rely on the recommended values for  $h_c$  developed for use with specific air models (Fisher and Pederson 1997) and user prescribed values. Ultimately a set of convection correlations should be developed/tested for use with air models. Such correlations can be a function of mass flow rate (mean velocity) in the adjacent air control volume, as well as the usual temperature difference, orientation, and length scales. For nodal models, the adjacent air control volume is larger and so current convection correlations are probably suitable.

### Air System Flow Rate

Without the well-mixed assumption there is not necessarily a unique solution for air system flow rate that meets load and comfort requirements. The two coupling options discussed above—direct and indirect—are also grouped such that they determine air system flow rates by different methods. With room air models, we can write

$$\dot{V} = \frac{\dot{Q}_{sys}}{\rho c_p (T_{Supply} - T_{Leaving})}, \quad (6)$$

where

- $\dot{V}$  = air system volume flow rate,
- $\rho$  = air density,
- $c_p$  = specific heat capacity of air at constant pressure,
- $T_{supply}$  = supply air temperature, and
- $T_{leaving}$  = air temperature going into the returns.

Note that with air models we expect  $T_{leaving}$  to have values that usually differ from  $T_{setpoint}$ . For this reason, Equation 6 for use in a poorly mixed thermal zone does not have the same predictive capability as it does for a well-mixed and controlled zone (where  $T_{setpoint} = T_{leaving}$ ). The system flow could be too much or too little for  $T_{statDB}$  to equal  $T_{Setpoint}$ .

In indirect coupling, the previous iteration's value for  $T_{leaving}$  is used, and model results are (hopefully) dragged together after iteration by applying deviations between  $T_{statDB}$  and  $T_{Setpoint}$

in the load/energy routines. However, with indirect coupling,  $T_{statDB}$  (predicted by air model) is not required to match  $T_{setpoint}$ , which allows using air models that do an adequate job of predicting *patterns* of temperature distribution without requiring accurate results for absolute temperatures.

In direct coupling, a so-called secondary system air iteration loop models  $\dot{V}$  as a function of  $T_{statDB}$ . The loop maintains room temperature control as a “real thermostat” would by adjusting  $\dot{V}$  up or down depending on deviations between  $T_{setpoint}$  and  $T_{statDB}$ . This secondary loop runs inside the main iteration loop and uses constant values for parameters from the surface domain while making additional calls to the air model. Before entering the loop, an initial prediction of  $\dot{V}$  is made using Equation 6 and the current value for  $T_{leaving}$ . The basic idea for a cooling situation is to increase system flow if  $T_{statDB}$  is too high and decrease flow if  $T_{statDB}$  is too low. This investigation implements a simple proportional controller where the gain is obtained by differentiating Equation 6.

Air system control can also be a function of additional comfort parameters such as radiant temperatures, air velocity, or humidity that might be expressed as some operative temperature,  $T_{op}$ . Equation 7 shows a crude method of modeling a value for the operative temperature,  $T_{op}$ , that was tested where the mean radiant temperature,  $T_{MRT}$ , is included, though clearly other relations could be used (such as weighting by radiative and convective heat transfer coefficients). This operative temperature control is implemented as an option in the toolkit.

$$T_{op} = \frac{1}{2}(T_{MRT} + T_{statDB}) \quad (7)$$

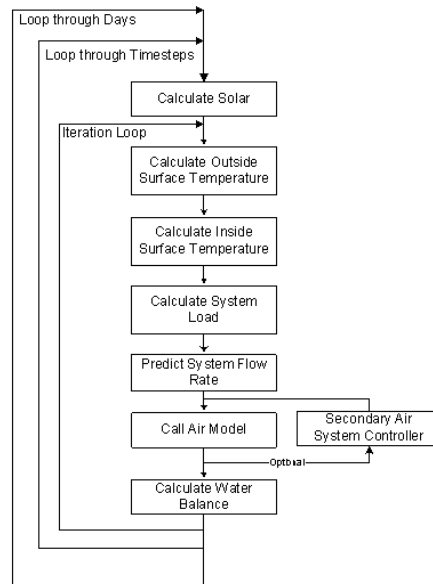
If there is reason to distrust the capability of the air model to accurately predict  $T_{statDB}$ , or if predictions are not sensitive to variations in the system flow rate, then the secondary system iteration loop is likely to fail. This extra loop also requires that extra calls be made to the air model, and this may be computationally expensive. Another category of problems may arise because it is possible that there are multiple solutions for  $\dot{V}$  where  $T_{statDB}$  is near  $T_{setpoint}$ . When these problems are present, the indirect-coupling method may be preferable because it does not require the secondary system air iteration loop.

### Solution Algorithm

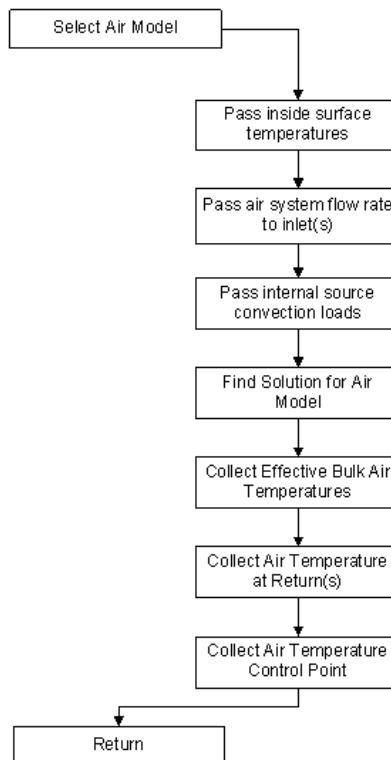
The iterative, or successive, substitution heat balance solution method is selected to find solutions to the heat balance model equations. Figure 3 diagrams how to implement such a coupled model in the context of a design-day calculation. Here the outermost day loop is for finding a steady periodic solution by repeating the same design-day environmental conditions. The next loop moves through the time steps per day where the toolkits use 24 time steps per day for hour-by-hour simulations. The iteration loop runs at a single time step and is used to allow sequentially computing each of the primary variables. After revisiting each calculation many times, the effect is to find a solution that satisfies all the relationships.

Figure 4 diagrams the general steps involved in the “call air model” step shown in Figure 3. This encompasses the steps involved in passing data to and from the air model as well as evaluating the entire model itself. Some models may also receive other types of data not indicated. For example, a call to the Mundt model (1996) will also receive the current value for  $\dot{Q}_{sys}$ . In this project, the focus is on “tightly coupled” models where the air model is computed with the same frequency as the primary variables in the surface domain.





**Figure 3. Iterative calculation strategy for coupled air and heat balance models.**



**Figure 4. General steps in calling an air model.**

## RESULTS AND DISCUSSION

Three cases are selected to show example results from implementing the framework. The first case is a steady-state validation exercise. The second is a numerical exercise for an office cooling load calculation. The third case is a steady-state numerical exercise used to study the sensitivity of model input parameters.

### Steady-State Validation

Validation is always difficult for building simulation, and the problem is not made easier with the addition of air modeling. Adding detailed data on the distribution of air temperatures to the usual requirements for validating dynamic building simulations makes high-quality data all the more scarce. Therefore, validation exercises are currently limited to steady-state situations. An example of such an exercise is presented that corresponds to measurements of side-wall displacement ventilation conducted by Li et al. (1993). The inside size of the chamber is 4.2 m by 3.6 m by 2.75 m in height. The total 300 W load is generated by operating electric resistance elements inside a porous box measuring 0.4 m by 0.3 m by 0.3 m that is filled with aluminum chips to distribute heat and inhibit radiative exchange. This internal source was modeled with splits of 75% convection and 25% radiation, by assumption. Temperature-controlled regions “outside” guard the chamber in order to establish steady-state conditions. The experiment had a constant air system flow rate and supply air temperature. The Mundt (1996) model used  $h_c$  values of 5.0 (W/m<sup>2</sup>·K) for the floor and ceiling surfaces. Rees and Haves (2001) also studied this case and developed  $h_c$  values of 8.51 W/m<sup>2</sup>·K for the ceiling, 6.06 W/m<sup>2</sup>·K for the floor, 1.3 W/m<sup>2</sup>·K for the lower walls, and 6.3 W/m<sup>2</sup>·K for the upper walls; these were used for both the zonal model from Rees (1998) and Rees and Haves (2001) and the momentum-zonal model (Griffith and Chen 2003).

For testing a cooling load calculation, we can imagine the simulation is of a variable air volume system, and the model “finds” the flow rate to meet  $T_{Setpoint}$  that was actually fixed in the experiment. A value for  $T_{Setpoint}$  was extracted from the measured air temperature data by interpolating between measured air temperature locations to obtain a value at 1.1 m from the floor. The surfaces are modeled as resistance constructions with Li’s values for a U-factor of 0.36 (W/m<sup>2</sup>·K) for all surfaces except the west wall, which had a U-factor 0.15 (W/m<sup>2</sup>·K). Table 1 shows the “outside” boundary conditions for testing the coupled air and loads models.

Table 2 lists overall results for this case using the coupled air and load routines. Figure 5 compares the results using the indirect-coupling method. Agreement between predicted and measured air temperatures is fairly good for all the air models, especially in the occupied zone. The well-mixed model performs adequately. In general we find that the coupled models have only a small effect on the result for  $\dot{Q}_{sys}$  but do have a significant effect on the air system temperature difference ( $T_{leaving} - T_{supply}$ ). The results indicate that (for this case) the Mundt model overpredicted the temperature at the outlet leading to a system flow rate that is too low. The Rees and

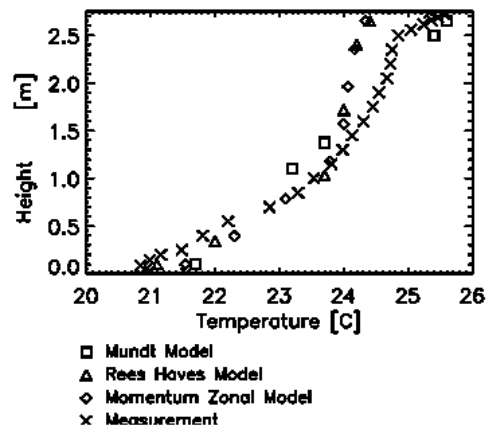
**Table 1. Coupled Air and Surface Model Boundary Conditions**

	Value	Units
$\dot{Q}_{conv,s}$ (estimated splits)	225	(W)
$\dot{Q}_{rad,s}$ (estimated splits)	75	(W)
$T_{supply}$	18.0	(°C)
$T_{Setpoint}$	23.8	(°C)
Outside face (“TG”), east, north, west, and floor	22.63	(°C)
Outside face air (“TB”), south and ceiling	19.9	(°C)

**Table 2. Comparison of Overall Results for Coupled Air and Loads Model with Experimental Data from Li et al. (1993)<sup>a</sup>**

Case B3 (Li et al. 1993)	$\dot{Q}_{sys}$ [W]	$\dot{V}$ [m <sup>3</sup> /s]	$T_{sysDiff}$ [C]	$T_{leaving}$ [C]	$T_{statDB}$ [C]
Measured data	-285	(0.035)	6.8	24.8	23.77
Well-mixed model	-247	0.036	5.8	(23.77)	(23.77)
Mundt model (indirect coupling)	-237	0.0269	7.4	25.44	23.29
Mundt model (direct coupling)	-232	0.023	8.5	26.5	23.77
Rees and Haves model (indirect coupling)	-253	0.034	6.3	24.3	23.77
Momentum-zonal model (indirect coupling)	-253	0.035	6.2	24.2	23.77
Momentum-zonal model (direct coupling)	-252	0.035	6.2	24.2	23.72

a. Values in parentheses are model inputs rather than results

**Figure 5. Indirect coupled air and load routine results for air temperatures: case B3 (Li et al. 1993).**

Haves model used 11 nodes and 14 flow paths, with flow rate parameters developed for this specific case (Rees and Haves 2001) rather than the general rules. The momentum-zonal model used a grid size of 9 by 8 by 9. It is encouraging that the models are able to obtain nearly the same airflow rate as used in the experiment. The too low values for  $\dot{Q}_{sys}$  probably stem from the choice of internal load splits (Rees [1998] considered a split of 100% convection suitable because of the low emittance materials). The Mundt model performed poorly with indirect coupling because the linear model does a poor job of predicting temperatures at the height of the thermostat.

## Office Cooling Load

The second case models a medium-sized office space at cooling design-day conditions for Sacramento, CA. The room simulated is an open-plan office for seven occupants and is 8 m by 8 m with an interior height of 2.74 m. The space is conditioned using side-wall displacement ventilation. The internal load schedules are patterned after energy modeling practice for a day-shift schedule, with maximum loads of about 35 W/m<sup>2</sup> and splits of 50% convection and 50% radiation. The west wall has stone on the lower portion and is entirely glazed above with low-shading-coefficient insulated glazing units. The south wall is stone veneer on metal framing and was exposed to outside air but has no windows. Vertical surfaces were subdivided into four segments. The Rees and Haves model (2001) used the suggested “rules” for path airflow rates and the  $h_c$  correlation for the lowest walls and used 3.0 W/m<sup>2</sup>·K for upper vertical wall surfaces and 5.9 W/m<sup>2</sup>·K for ceiling surfaces. The other models used default surface convection film coefficients from the toolkit (4.68 W/m<sup>2</sup>·K for the vertical walls, 1.25 W/m<sup>2</sup>·K for the ceiling, and 4.37 W/m<sup>2</sup>·K for the floor). The momentum-zonal model used nonblocking interior objects with internal sources distributed uniformly among the objects.

Figure 6 shows overall cooling load calculation results using the well-mixed model and three different air models with a constant room air setpoint of 22.8°C, supply air temperature of 17.2°C, and indirect coupling method. Although cooling load results are similar, results for air system flow rates vary because of differences in model predictions for  $T_{leaving}$ . Figure 7 shows

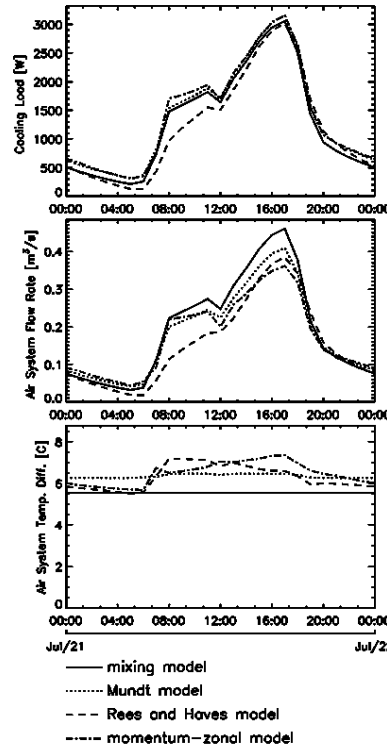
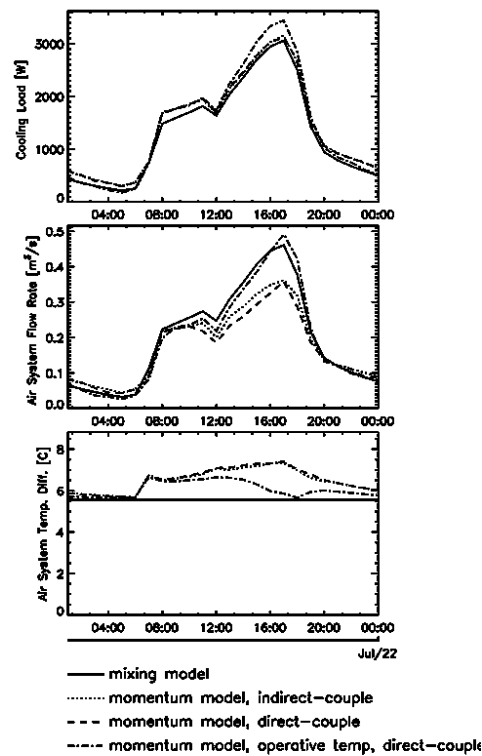


Figure 6. Office load calculation results for  $\dot{Q}_{sys}$ ,  $\dot{V}$ , and  $T_{sysDiff}$  for different air models and constant room air setpoint.



**Figure 7. Momentum-zonal model results for  $\dot{Q}_{sys}$ ,  $T_{sysDiff}$ , and  $\dot{V}$  with three air system control strategies.**

the same case with the momentum-zonal air model and different air system control strategies. The direct and indirect coupling methods had essentially the same results when based on the air model prediction for  $T_{statDB}$ . Direct coupling, but with control based on an operative temperature that includes radiative conditions (defined in Equation 7), leads to a quite different overall solution with 10% higher cooling loads and a 37% increase in air system flow rate compared to the same model with only air dry-bulb control. The increases can be understood by considering that if surfaces are warmer than the setpoint (as they are likely to be because of radiative gains), the air system will cool the air below setpoint, resulting in larger air temperature differences. It is interesting that the prediction for  $\dot{V}$ , with  $T_{op}$ -based control and detailed air modeling, matches the traditional well-mixed model's prediction for  $\dot{V}$ . ( $T_{op}$ -based control was not implemented for the well-mixed model.) This example shows that such methods for controlling  $\dot{V}$  may be important to fully characterize designs that attempt to use thermal stratification to improve efficiency since allowing temperatures to elevate (outside of occupied zone) may, in practice, lead to different air system flow/settings to attain comparable thermal comfort.

The time required for computations increased by about a factor of four for the nodal models compared to the well-mixed model. For the momentum-zonal model with a grid number of 216, the increase in computation time was about a factor of 100 longer than the well-mixed model.

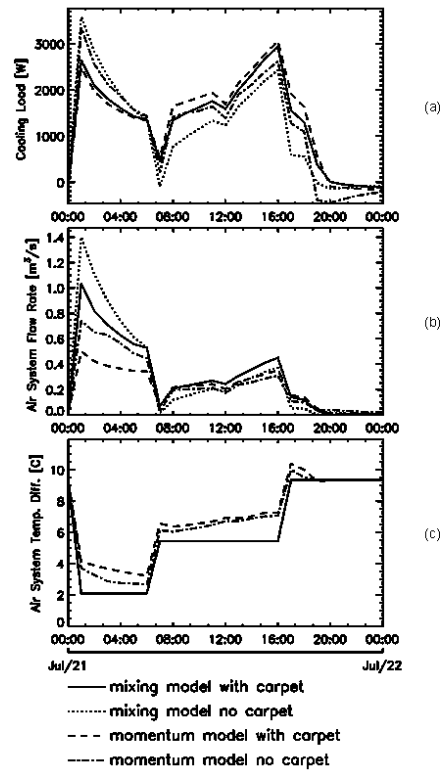


**Figure 8.** Office load calculation results for  $\dot{Q}_{sys}$ ,  $\dot{V}$ , and  $T_{sysDiff}$  for well-mixed and momentum air models with and without carpet, moderate pre-cool setpoint strategy.

Nonconstant room air temperature setpoint strategies are also investigated in order to assess how coupled air and load models respond when simulating diurnal thermal mass storage strategies. Is heated air being extracted before it has a chance to warm the building mass? A room air setpoint strategy termed “moderate pre-cool” was taken from the work of Braun et al. (2001). Here the idea is to cool off the building thermal mass in the morning hours to lower cooling load during peak hours. Exposing the thermal mass of concrete floor slabs to the zone air is a recognized technique for increasing thermal inertia in low-energy design (see, for example, Gratia and De Herde [2003]). Therefore, a simulation exercise was conducted to model the effect of carpet on the concrete floor slab. Figure 8 shows the results with and without carpet for the well-mixed model and the momentum model using the moderate pre-cool setpoint strategy. For the well-mixed model, the afternoon peak cooling load reduction by removing the carpet was 17% and, for the momentum model, the reduction was 22%.

Figure 9 plots data from the same simulations shown in Figure 8 but in a much different way. Figure 9 shows the ratio of the overall cooling loads from the two models versus deviations in near-surface air temperatures between the momentum air model and the well-mixed model. Figure 9a can explain why air models do not always affect cooling loads since the values for  $T_a$  shift both up and down with respect to those of the well-mixed model (even scatter around 0.0 on x-axis). In many cases, this appears to roughly balance out, resulting in little change in the net

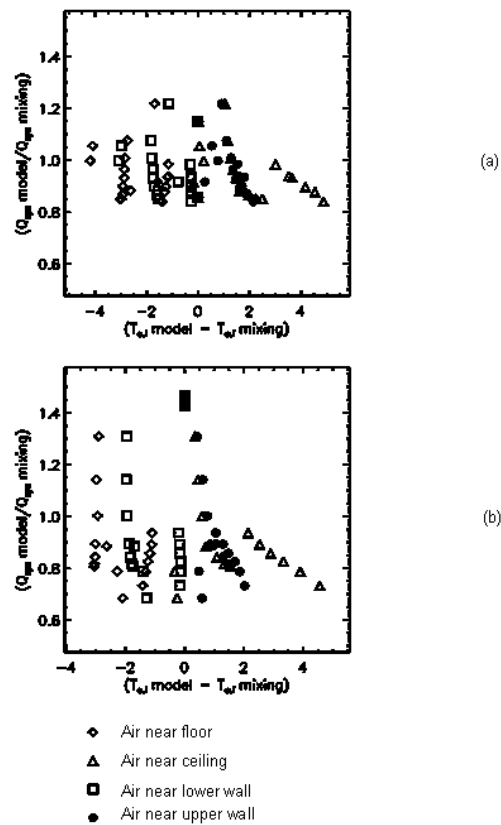


**Figure 9. Ratio of change in  $\dot{Q}_{sys}$  with momentum-zonal air model to  $\dot{Q}_{sys}$  with well-mixed model as a function of deviations in  $T_{a,i}$  (a) with carpet and (b) without carpet.**

cooling load. However, Figure 9b shows qualitative differences in that heat load ratios cluster further below 1.0 than do the data of Figure 9a. The only difference between Figures 9a and 9b is the presence of carpet on the floor slab. This supports the assertion that improved detail in thermal zone modeling is helpful for strategies that make better use of the building thermal mass.

### Sensitivity of Inside Face Surface Temperature to Modeling Parameters

An important outcome of coupling air and load models is that results for surface temperature at the inside face differ from those using the well-mixed model. Even if results for overall cooling load depend only slightly on the thermal resistance of convection, results for surface temperature can be strongly affected by how surface convection heat transfer is modeled at the inside face. If the room air exhibits thermal stratification, then lower surfaces will tend to be cooler and upper surfaces will tend to be warmer than results using the well-mixed model. Improving results for surface temperature may be of interest regardless of the overall impact on load or energy if controls are based on the radiative environment or when the model is part of an evaluation of thermal comfort or condensation.

This section presents results for temperatures of selected surfaces and adjacent-air control volumes obtained during simple parametric investigations of certain modeling parameters (user input). These parameters include the convection film coefficient,  $h_c$ , the thickness of the adjacent-air control volumes,  $t_{CV}$ , and the resolution used when subdividing surfaces in the surface/load domain. A full investigation and development of clear guidelines for these input parameters, for all types of thermal zones that one might encounter, is beyond the scope of the current research project.

A third test case, referred to as “virtual thermal test chamber,” or VTTC, models a steady-state thermal test chamber with controlled/guarded inside surfaces on five sides and a sixth vertical wall surface exposed to a climate chamber. This “thermal test specimen” wall is the focus of a brief investigation. The case is designed to suggest laboratory thermal experiments that would be useful for validating coupled models. The chamber is a simple box with an inside size of 3.75 m deep, 3.25 m wide, and 2.75 m high. “Outside” temperatures are steady-state at 36.9°C for cooling. There is no incident solar radiation. The five controlled/guarded surfaces are modeled as thin sheet metal plenums with outside faces exposed to air at the same temperature as the room air setpoint. The intent is to expose the surface being analyzed to similar radiative forcing between parametric runs so that surface temperature fluctuations will arise mostly from differences in convection surface heat transfer rather than differences in radiation.

The test case has no infiltration, and two underfloor air distribution inlets provide cooling air at 17.2°C (VAV control). Room air setpoint is 22.8°C. In these virtual cooling experiments, electrically heated blinds are situated next to the glazing to simulate heating from absorbed solar on window blinds (146 W of convective load). Other internal loads consist of an overhead lighting fixture (9.0 W/m<sup>2</sup>), one person, and one PC (36 W convective load).

### Surface Convection Heat Transfer Coefficient and Adjacent-Air Control Volume Size

The momentum-zonal model was used to explore how variations in  $h_c$  and  $t_{CV}$  affect results for temperatures. These parameters are presented together since they are interconnected. A grid of  $10 \times 10 \times 8$  was used for all of the simulations in this section. The thermal test wall in these cases consists of clear double glazing and opaque sections of stone veneer, steel framing, R<sub>IP</sub>-11 batt insulation, and wallboard. Glazing area is about 57% with glazings running in a band across the entire east wall. The sensitivity of the arbitrary “0.1 m rule” is explored by using three different grid arrangements. Boundary cell sizes (normal to surface) of 0.1, 0.2, and 0.3 m were used with the remaining interior cells uniformly distributed across the domain. This corresponds to investigating a “0.05 m rule” and a “0.15 m rule,” as well as the “0.1 m rule” since we consider a boundary cell’s temperature to be a model of the value at the center of the control volume. Table 3 lists how a set of values for  $h_c$  was modified by a simple function,  $f(h_c)$ . The case was run for all permutations of boundary cell size and film coefficient.

**Table 3. Function  $f(h_c)$  Values for Surface Convection Heat Transfer Coefficients**

$f(h_c)$	$h_c$ mid and upper walls (W/m <sup>2</sup> ·K)	$h_c$ lower walls (W/m <sup>2</sup> ·K)	$h_c$ ceiling (W/m <sup>2</sup> ·K)	$h_c$ floor (W/m <sup>2</sup> ·K)	$h_c$ glazing (W/m <sup>2</sup> ·K)
0.50	1.50	1.05	2.95	2.0	2.34
0.75	2.25	1.58	4.43	3.0	3.51
1.00	3.00	2.10	5.90	4.0	4.68
1.25	3.75	2.63	7.38	5.0	5.85
1.50	4.50	3.15	8.85	6.0	7.02



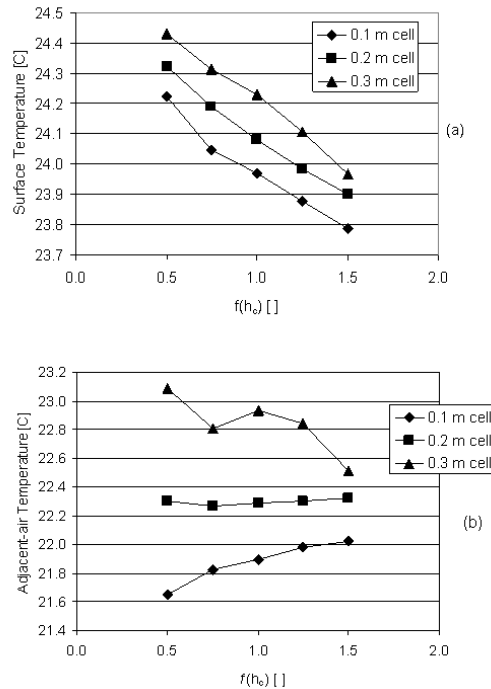


**Figure 10. Variation in (a) surface and (b) adjacent-air temperatures for a lower insulated wall (adding heat to air) with different input levels for  $h_{c,i}$ 's and  $t_{CV}$ , case VTTC\_cooling  $10 \times 10 \times 8$  momentum-zonal air model.**

Figure 10 shows temperature results for a lower insulated surface, and Figure 11 shows results for an upper glazing panel for the VTTC test case with a steady room air setpoint of  $22.8^\circ\text{C}$  and climate chamber at  $36.9^\circ\text{C}$ . The coupling strategy for these is direct coupling. The cases in the series with 0.3 m and 0.2 m boundary cells showed problems with the secondary air system control loop where multiple solutions were obtained by the controller. This did not allow the simulation to converge to steady state. Further investigation is needed to explore dampening this instability. This is the reason for the lack of clear trends in the 0.2 and 0.3 m data in Figure 11.

Results for adjacent-air temperature were found to vary more strongly with boundary cell size than with surface heat transfer coefficient, as shown by the relatively flat curves for adjacent-air temperature. This is expected since the overall heat flow is not strongly affected by  $h_c$  since it is a relatively small part of the overall thermal resistance. A larger cell volume distributes heat loss or gain over more mass and, thus, temperatures are closer to the surface temperature for smaller cells. Air temperature results varied by as much as  $1.5^\circ\text{C}$  for the different input settings.

Results for inside face surface temperatures show a strong dependence on values for  $h_c$ . As expected, the effect is much stronger for the more poorly insulated clear double glazing than for the insulated building wall. Glazing temperatures varied  $1^\circ\text{C}$  under cooling conditions for the different input values. Insulated wall temperatures varied by  $0.6^\circ\text{C}$ . There are multiple combinations of  $h_c$  and cell size that can produce the same result for surface temperature. The trends support the discussion above, asserting that smaller adjacent-air control volumes lead to higher values for  $h_c$ .

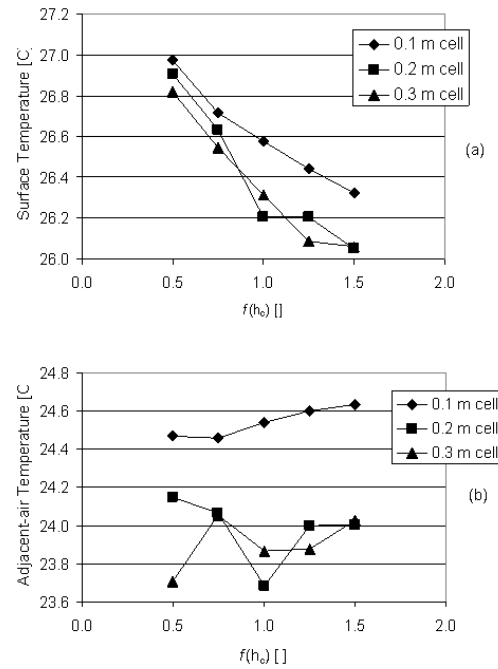


**Figure 11. Variation in (a) surface and (b) adjacent-air temperatures for an upper glazing panel (adding heat to air) with different input levels for  $h_{c,i}$ 's and  $t_{CV}$ , case VTTC\_cooling  $10 \times 10 \times 8$  momentum-zonal air model.**

A comparison of simulation results cannot provide a clear determination or recommendation of the appropriate combination of  $h_c$  and boundary cell size. Measured data are needed to characterize what modeling strategy produces the most realistic results. Significant additional research is required to develop methods of determining  $h_c$  values and boundary cell sizes that are appropriate for a wide variety of building types and thermal situations.

### Vertical Resolution of Surfaces

A wall may be subdivided in the vertical direction so that surface modeling can account for variations in the adjacent-air temperature that might arise from thermally stratified air conditions. For this parametric analysis, the thermal test specimen (or east wall of the VTTC) was changed to a homogenous construction of clear double glass and modeled with the baseline  $h_c$  values ( $f/h_c = 1.0$ ) and cell size ( $t_{CV} = 0.2$ ). Separate test cases subdivided the test wall into 1, 2, 3, 4, 6, and 8 individual plates.

Figure 12 presents results for temperatures along the vertical direction of the test wall. All of the different resolutions are consistent with each other in that they describe a similar profile. It is difficult to draw conclusions about what level of subdividing is most appropriate. The data show that increasing resolution provides more detail to the temperature profile and better values for temperature extremes. The decision to increase vertical resolution would probably be made because of a need to know extremes of surface temperature. Future model development that incorporates more detailed radiation exchange may also play a role in determining appropriate levels of subdividing.

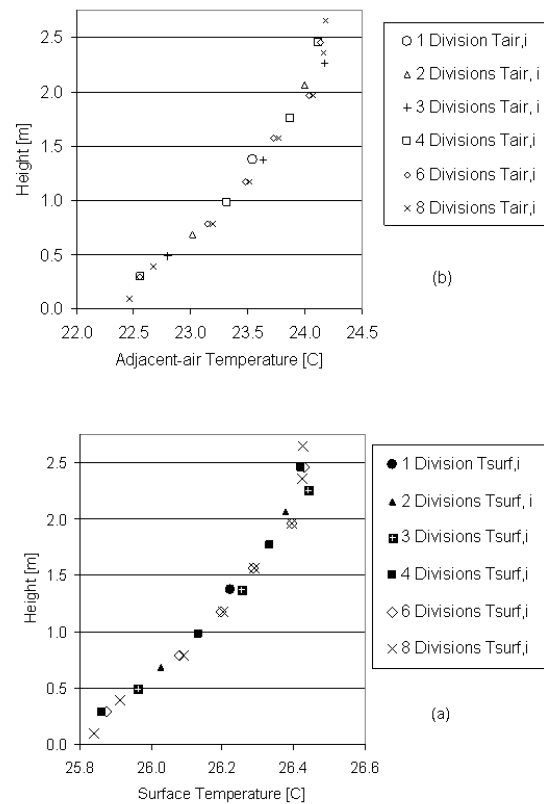


**Figure 12. Results for (a) adjacent-air and (b) surface temperatures for different levels of subdividing a vertical double-glazed facade and  $10 \times 10 \times 8$  momentum-zonal air model.**

## CONCLUSIONS

This study has developed a framework and implemented computer code in an ASHRAE toolkit for coupling room air models and heat balance-based load calculations. The load calculations used the successive substitution iterative technique implemented by Pedersen et al. (2001). The code and model formulation were altered to accept zone air temperature as an array of values so that surfaces, returns, and a thermostat can use values for air temperature that differ from the room setpoint. Applications for such modeling are where the room air is stratified. The temperature distributions are generated using room air models of the type known as nodal and zonal. Two models were selected from the literature and implemented in computer programs in order to demonstrate and test the coupling framework. These are the Mundt (1996) model and the Rees and Haves (2001) nodal model. A third model termed “momentum-zonal” was developed that uses finite-volume techniques to solve the Euler flow equation in three dimensions.

The model-coupling framework and code appear to perform well, although adequate validation data are not available. The toolkit contains a versatile test program that performs detailed, hourly load calculations for a single thermal zone where both network and three-dimensional airflow models have been tightly coupled to the load routines. This research focused on sensible load calculations, but room air modeling is also considered useful for evaluating thermal comfort and indoor air quality. For these purposes, the toolkit’s coupling framework provides a ther-

mal envelope calculation engine that generates useful boundary conditions for surface temperatures and system flow rates that should aid detailed modeling of the indoor environment.

It appears practical to use room air models to predict the air temperature at the location of the thermostat and where it enters the returns in order to provide more detail on how the thermal zone is represented to system and plant models. However, multiple solutions for system airflow rates are possible and can lead to instabilities that need further investigation. Results from cooling load calculations using the complete well-mixed model have been compared to those using the room air models. When room setpoints were constant, predictions showed only minor changes to the overall cooling load, indicating that the well-mixed model does an adequate job of determining system loads. For displacement ventilation, the air models showed consistent and significant changes to the predicted air system flow rate and return air temperatures. This allows load and energy calculations to account for the higher heat extraction efficiency offered by displacement ventilation. In one test case, system flow rate reductions of around 25% were obtained, which could have important implications for fan energy and sizing air distribution equipment. Altering return air temperatures will also affect plant/economizer thermodynamics. The results for individual surfaces do vary with the additional modeling detail but, in aggregate, losses and gains often even out. An alternative strategy for air system control based on an operative temperature that includes mean radiant temperature showed a 10% effect on cooling load and a 37% effect on system flow rate. However, when intentionally scheduling room air temperatures to take advantage of diurnal thermal mass in the building surfaces, the air models were found to have a larger affect on the overall cooling loads.

The time required for computations increased by a factor of about four for the nodal models compared to the well-mixed model. Nodal models could be added to whole building simulations with moderate additional computation time required and could be expected to improve predictions of flow rate and return air temperatures experienced by the plant. For the momentum-zonal model with a grid number of 216, the increase in computation time was about a factor of 100 longer than the well-mixed model. Incorporating a three-dimensional, coarse-grid, air-modeling package into building simulation is feasible with contemporary computers, but it would require users to be very patient.

## REFERENCES

- Beausoleil-Morrison, I. 2000. The adaptive coupling of heat and air flow modeling within dynamic whole-building simulation, Ph.D. Thesis, University of Strathclyde, Glasgow U.K.
- Braun, J., K. Montgomery, and N. Chaturvedi. 2001. Evaluating the performance of building thermal mass control strategies. *International Journal of HVAC&R Research* 7(4):403-428.
- Chen, Q., and J. van der Kooi. 1988. ACCURACY—A computer program for combined problems of energy analysis, indoor airflow and air quality. *ASHRAE Transactions* 94(2):196-214.
- Chen, Q., and B. Griffith. 2002. Incorporating nodal room air models into building energy calculation procedures, Final Report for ASHRAE RP-1222, 207 pages, School of Mechanical Engineering, Purdue University, West Lafayette, Ind.
- EQUA. 2002. IDA Simulation Environment. Sundyberg, Sweden.
- Fisher, D., and C.O. Pedersen. 1997. Convective heat transfer in building energy and thermal load calculations. *ASHRAE Transactions* 103(2).
- Gratia, E., and A. De Herde. 2003. Design of low energy office buildings. *Energy and Buildings* 35(2003):473-491.
- Griffith, B., and Q. Chen. 2003. A momentum-zonal model for predicting zone airflow and temperature distributions to enhance building load and energy simulations. *International Journal of HVAC&R Research* 9(3):309-325.
- Haghighat, F., Y. Lin, and A.C. Megri. 2001. Development and validation of a zonal model—POMA. *Building and Environment* 36:1039-1047.

- Inard, C., H. Bouia, and P. Dalicieux. 1996. Prediction of air temperature distribution in buildings with a zonal model *Energy and Buildings* 24:125-132.
- Li, Y., M. Sandberg, and L. Fuchs. 1993. Vertical temperature profiles in rooms ventilated by displacement: full scale measurement and nodal modeling. *Indoor Air* 2:225-243.
- Mundt, E. 1996. The performance of displacement ventilation systems-experimental and theoretical studies, Ph. D. Thesis, Royal Institute of Technology, Stockholm.
- Negrao, C. 1995. Conflation of computational fluid dynamics and building thermal simulation, Ph.D. Thesis, University of Strathclyde, Glasgow, UK.
- Pedersen, C.O., D.E. Fisher, and R.J. Liesen. 1997. Development of a heat balance procedure for cooling loads. *ASHRAE Transactions* 103(2).
- Pedersen, C.O., R.J. Liesen, R.K. Strand, D.E. Fisher, L. Dong, and P.G. Ellis. 2001. A toolkit for building load calculations. Atlanta: American Society of Heating, Refrigerating and Air-Conditioning Engineers, Inc.
- Rees, S.J. 1998. Modeling of displacement ventilation and chilled ceiling systems using nodal models, Ph.D. Thesis, Loughborough University.
- Rees, S.J., and P. Haves. 2001. A nodal model for displacement ventilation and chilled ceiling systems in office spaces. *Building and Environment* 36:753-762.
- Sowell, E. 1991. A general zone model for HVACSIM+ user's manual, Report No. OUEL 1889/91, University of Oxford, Oxford, UK.
- Spitler, J.D., C.O. Pedersen, D. Fisher, P.F. Menne, and J. Cantillo. 1991a. An experimental facility for investigation of interior convective heat transfer. *ASHRAE Transactions* 97(1).
- Spitler, J.D., C.O. Pedersen, and D. Fisher. 1991b. Interior convective heat transfer in buildings with large ventilative flow rates. *ASHRAE Transactions* 97(1).
- Srebric, J., Q. Chen, and L.R. Glicksman. 2000. A coupled airflow-and-energy simulation program for indoor thermal environment studies. *ASHRAE Transactions* 106(1):465-476.
- Walton, G. 1993. Computer programs for simulation of lighting/HVAC interactions, NISTIR 5322. National Institute of Standards and Technology.
- SPARK, 1997. SPARK 1.0.1 reference manual: simulation problem analysis and research kernel, Lawrence Berkeley National Laboratory, Ares Sowell and Associates.
- Zhai, Z., Q. Chen, P. Haves, and J.H. Klems. 2002. On approaches to couple energy simulation and computational fluid dynamics programs. *Building and Environment* 37:857-864.
- Zhai, Z., and Q. Chen. 2003. Solution characters of iterative coupling between energy simulation and CFD programs. *Energy and Buildings* 35(2003):493-505.

